World Journal of

Diabetes

World Journal of *Diabetes*

Contents

Contents

ABOUT COVER

Editorial Board Member of *World Journal of Diabetes*, Da Li, MD, PhD, DSc (Med), Professor, Deputy Director, Center of Reproductive Medicine, Shengjing Hospital of China Medical University, Shenyang 110004, Liaoning Province, China. leeda@ymail.com

AIMS AND SCOPE

The primary aim of *World Journal of Diabetes* (*WJD*, *World J Diabetes*) is to provide scholars and readers from various fields of diabetes with a platform to publish high-quality basic and clinical research articles and communicate their research findings online.

  WJD mainly publishes articles reporting research results and findings obtained in the field of diabetes and covering a wide range of topics including risk factors for diabetes, diabetes complications, experimental diabetes mellitus, type 1 diabetes mellitus, type 2 diabetes mellitus, gestational diabetes, diabetic angiopathies, diabetic cardiomyopathies, diabetic coma, diabetic ketoacidosis, diabetic nephropathies, diabetic neuropathies, Donohue syndrome, fetal macrosomia, and prediabetic state.

INDEXING/ABSTRACTING

The *WJD* is now abstracted and indexed in Science Citation Index Expanded (SCIE, also known as SciSearch®), Current Contents/Clinical Medicine, Journal Citation Reports/Science Edition, PubMed, and PubMed Central. The 2021 Edition of Journal Citation Reports® cites the 2020 impact factor (IF) for *WJD* as 3.763; IF without journal self cites: 3.684; 5-year IF: 7.348; Journal Citation Indicator: 0.64; Ranking: 80 among 145 journals in endocrinology and metabolism; and Quartile category: Q3.

RESPONSIBLE EDITORS FOR THIS ISSUE

Production Editor: *Rui-Rui Wu*; **Production Department Director:** *Xu Guo*; **Editorial Office Director:** *Jia-Ping Yan.*

ORIGINAL ARTICLE

Basic Study

Roles of transient receptor potential channel 6 in glucose-induced cardiomyocyte injury

Shi-Jun Jiang

Shi-Jun Jiang, School of Basic Medicine, Huazhong University of Science and Technology, Wuhan 430030, Hubei Province, China

Corresponding author: Shi-Jun Jiang, MM, Research Fellow, School of Basic Medicine, Huazhong University of Science and Technology, No. 13 Aviation Road, Qiaokou District, Wuhan 430030, Hubei Province, China. jiangsj_89756@163.com

Abstract

BACKGROUND

Diabetic cardiomyopathy (DCM) is a serious complication of end-stage diabetes that presents symptoms such as cardiac hypertrophy and heart failure. The transient receptor potential channel 6 (TRPC6) protein is a very important selective calcium channel that is closely related to the development of various cardiomyopathies.

AIM

To explore whether TRPC6 affects cardiomyocyte apoptosis and proliferation inhibition in DCM.

METHODS

We compared cardiac function and myocardial pathological changes in wild-type mice and mice injected with streptozotocin (STZ), in addition to comparing the expression of TRPC6 and P-calmodulin-dependent protein kinase II (P-CaMKII) in them. At the same time, we treated H9C2 cardiomyocytes with high glucose and then evaluated the effects of addition of SAR, a TRPC6 inhibitor, and KN-93, a CaMKII inhibitor, to such H9C2 cells in a high-glucose environment.

RESULTS

We found that STZ-treated mice had DCM, decreased cardiac function, necrotic cardiomyocytes, and limited proliferation. Western blot and immunofluorescence were used to detect the expression levels of various appropriate proteins in the myocardial tissue of mice and H9C2 cells. Compared to those in the control group, the expression levels of the apoptosis-related proteins cleaved caspase 3 and Bax were significantly higher in the experimental group, while the expression of the proliferation-related proteins proliferating cell nuclear antigen (PCNA) and CyclinD1 was significantly lower. *In vivo* and *in vitro*, the expression of TRPC6 and P-CaMKII increased in a high-glucose environment. However, addition of inhibitors to H9C2 cells in a high-glucose environment resulted in alleviation of

both apoptosis and proliferation inhibition.

CONCLUSION
The inhibition of apoptosis and proliferation of cardiomyocytes in a high-glucose environment may be closely related to activation of the TRPC6/P-CaMKII pathway.

Key Words: Diabetic cardiomyopathy; Apoptosis; Proliferation; H9C2 cells; Transient receptor potential channel 6; P-calmodulin dependent protein kinase II

Core Tip: Diabetic cardiomyopathy is a serious complication of end-stage diabetes that presents symptoms such as cardiac hypertrophy and heart failure. The transient receptor potential channel 6 (TRPC6) protein is a very important selective calcium channel that is closely related to the development of various cardiomyopathies. We found that the inhibition of apoptosis and proliferation of cardiomyocytes in a high-glucose environment might be closely related to the activation of the TRPC6/P-calmodulin-dependent protein kinase II pathway.

INTRODUCTION

Diabetes is a disorder of glucose metabolism that is characterized by elevated blood glucose levels[1,2]. A serious complication of diabetes is diabetic cardiomyopathy (DCM), which can cause extensive necrosis of myocardial tissue, eventually resulting in heart failure and even cardiogenic shock[1,2]. The pathological manifestations of DCM are different from myocardial necrosis caused by ischemia and hypoxia of coronary heart disease or myocardial hypertrophy caused by simple hypertension. DCM is an independent and specific myocardial disease characterized by myocardial collagen precipitation and interstitial fibrosis. Cardiomyocyte apoptosis and a large amount of fibrous tissue proliferation are important manifestations of DCM[3-5], accompanied by over-activation of the renin angiotensin system (RAS)[6] and an increase in oxygen free radicals[7].

The RAS in the myocardium regulates cardiovascular function and promotes the growth of cardiomyocytes and vascular smooth muscles under normal conditions[8]. In a high-glucose (HG) environment, an increase in angiotensin II (AngII) in the RAS system results in an increase in the secretion of mineralocorticoid aldosterone, thereby causing an increase in the cardiac load[9]. Excessive secretion of cardiovascular endothelin can directly produce vasoconstrictors, induce vascular smooth muscle proliferation, and accelerate myocardial damage[10]. Simultaneously, endothelin stimulates the proliferation of myocardial fibroblasts and changes collagen metabolism, causing myocardial interstitial remodeling and affecting cardiac systolic and diastolic functions[11]. The increase in oxygen free radicals [reactive oxygen species (ROS)] is another important cause of myocardial damage in the HG environment. In diabetes, the level of lipid superoxide in muscle tissue increases significantly[12], while the expression of ROS-scavenging enzymes such as catalase and superoxide dismutase (SOD) in the myocardium is relatively low. Cardiomyocytes can easily become the target group of oxidative radicals and reactions. An *et al*[13] and Boyer *et al*[14] have shown that the use of antioxidants has a protective effect on myocardial cells in DCM, in addition to greatly improving the functional and morphological indexes of myocardial cells in DCM.

Canonical transient receptor potential channel 6 (TRPC6) is a non-selective cationic calcium channel protein with a molecular weight of 106 kDa[15]. As an important member of the transient receptor potential protein family, TRPC6 protein is expressed in various tissues such as the lung, heart, kidney, skin, and vascular system[16-19], and plays an important role in the physiological and pathophysiological processes of various cells. Apoptosis is a form of cell death and intracellular calcium overload is an important factor that triggers apoptosis[20]. Myocardial ischemia-reperfusion studies have found that selective knockout of TRPC6 can significantly reduce the degree of cardiomyocyte apoptosis and ischemia-reperfusion injury[21], suggesting that knockout of TRPC6 may inhibit ischemia-reperfusion-induced cardiomyocyte apoptosis, by inhibiting calcium influx. Calmodulin-dependent protein kinase II (CaMKII) is widely distributed in various tissues and cells, and is closely related to various life activities related to Ca^{2+}. In recent years, many studies have reported that CaMKII

plays an important role in various myocardial diseases, such as myocardial hypertrophy, myocardial infarction, and arrhythmia[22,23]. However, there are few reports on the interaction between TRPC6 and CaMKII, which warrants further research.

DCM pathogenesis is often related to the inflammatory process triggered by AngII, ROS, and extracellular regulated kinase (ERK)[24], suggesting that TRPC6 may be involved in DCM pathogenesis. Therefore, in the present study, a streptozotocin (STZ)-induced DCM mouse model was constructed to detect the expression of apoptosis-related proteins, including Bax, cleaved caspase 3 (CC3), and Bcl-2, and proliferation-related proteins, including proliferating cell nuclear antigen (PCNA) and CyclinD1. In addition, the model was used to evaluate the level of cardiomyocyte injury in a HG environment, to further explore the mechanism of apoptosis and proliferation inhibition induced by the HG environment through the TRPC6/P-CaMKII pathway *in vitro*. This study aimed to clarify the pathophysiological mechanism of DCM and provide a theoretical basis for identifying new targets for DCM treatment.

MATERIALS AND METHODS

This study was approved by the Ethics Committee of Hubei Provincial Center for Disease Control and Prevention, and was conducted in accordance with the Declaration of Helsinki and the ARRIVE guidelines (https://arriveguidelines.org).

Reagents

Dimethyl sulfoxide (Sigma-Aldrich, United States), high-sugar Dulbecco's modified Eagle's medium (HyClone, United States), low-sugar Dulbecco's modified Eagle's medium (HyClone), Cell Counting Kit-8 (CCK-8; Beyotime, China), fetal bovine serum (Amresco, United States), radioimmunoprecipitation assay buffer (Amresco), protein concentration detection kit (Amresco), phenylmethyl sulfonyl fluoride (Amresco), cocktail protease inhibitor (Amresco), sodium dodecyl sulfate (SDS; Amresco), STZ (MedChemExpress, United States), KN-93 (MedChemExpress), Tween-20 (Amresco), SAR (Sigma-Aldrich), primary antibodies against TRPC6 (Abcam, United States), CC3 (Abcam), T-CAMKII (Abcam), P-CAMKII (Signalway Antibody, United States), Bcl-2 (Abcam), glyceraldehyde 3-phosphate dehydrogenase (Cell Signaling Technology, United States), Bax (Cell Signaling Technology), PCNA (Abcam), CyclinD1 (Cell Signaling Technology), and sheep anti-mouse secondary antibody (Abcam) were used in this study.

Experimental animals and protocol

Animal feeding: C57 mice were purchased from Changzhou Cavens Laboratory Animal Co., Ltd. Twenty male C57 mice aged 6–8 wk, with good vital signs, were selected and raised in a standard animal room, with a relatively stable temperature and humidity.

Modeling method: STZ solution (at a concentration of 6.5 mg/mL) was prepared in citric acid buffer (pH 4.5). After 5 h of fasting, mice in the experimental group were intraperitoneally injected with STZ solution (15 µL/g) and those in the control group were injected with an equal amount of citric acid buffer for 3 d. After 7 d, the non-fasting blood glucose levels of the mice in each group were measured. When the non-fasting blood glucose level of the STZ mice exceeded 17 mmol/L, the model was considered to be successfully established.

Blood glucose measurement: One week and four weeks after the last administration, the non-fasting blood glucose levels of the mice were measured using peripheral blood. The tail tip was cut off with scissors, following which their peripheral blood was collected, and glucose levels in it were measured using a blood glucose meter (Abbott), when the mice were in a stress-free state.

The mice were then placed under deep anesthesia and euthanized by means of cervical dislocation, following which their myocardial tissue was collected for the experiment.

Cell culture

H9C2 cells were donated by the Laboratory of Anesthesiology Department of Union Hospital Affiliated with the Huazhong University of Science and Technology. After passage, the cells were divided into five groups according to the different culture media and drugs used: Low-glucose (LG) group–LG medium at a concentration of 5.5 mmoL/L; control group–275 µL of mannitol solution at a concentration of 500 mmoL/L was added to 5 mL of LG medium at a concentration of 5.5 mmoL/L, to obtain an osmotic pressure of 33 mmoL/L, as measured using OsmoPRO (Advanced Instruments Inc.); HG group–275 µL of glucose solution at a concentration of 500 mmoL/L was added to 5 mL of LG medium at a concentration of 5.5 mmoL/L, to obtain an osmotic pressure of 33 mmoL/L, as measured using OsmoPRO; high-glucose plus TRPC6 inhibitor group (HG + SAR)–sar7332 at a final concentration of 2 µmol/L was added to the HG medium at a concentration of 33.3 mmol/L; high-glucose plus CaMKII inhibitor group (HG + KN-93)–KN-93 at a final concentration of 5 µmol/L was added to the HG

medium at a concentration of 33.3 mmol/L. After 72 h, subsequent experiments were performed.

Western blot analysis

Proteins extracted from the mouse myocardium or H9C2 cells were separated by means of 15% sodium dodecyl sulphate polyacrylamide gel electrophoresis (SDS-PAGE) and transferred to a polyvinylidene fluoride (PVDF) membrane. The PVDF membrane with proteins was placed in skimmed milk powder for sealing. Primary antibody (1:500 dilution) was evenly dropped onto the PVDF membrane, which was then incubated in a shaker at 4 °C overnight. The primary antibody was eventually aspirated and the membrane was rinsed. Goat anti-rabbit IgG or goat anti-mouse IgG was diluted at a ratio of 1:1000 and added to the PVDF membrane box, which was shaken on a shaking table for 1 h. The chemiluminescent solution was mixed, configured, and poured onto the PVDF film with a pipette. After that, the strip drenched with the luminescent solution was placed into the developer for development. Finally, the strip was analyzed using the Image Lab (Bio-Rad Laboratories) and ImageJ (National Institutes of Health) software.

Immunofluorescence

Cell specimens and tissue sections were fixed with 4% paraformaldehyde for 15 min at room temperature. The samples were then washed with PBS (pH 7.4, 0.1 moL/L) three times, for 8 min each time. Triton X-100 was prepared at a concentration of 0.1% in PBS, and the samples were incubated with it at room temperature for 15 min. The samples were then washed with PBS three times, for 8 min each, and incubated with 3% donkey serum at room temperature for 25 min. The slides were washed again with warm PBS for 8 min. According to the manufacturer's instructions, the samples were incubated with primary antibodies against PCNA (at a dilution of 1:200), TRPC6 (1:400), and CC3 (1:400), following which the samples were placed in a refrigerator at 4 °C overnight. The slides were rinsed with PBS three times, for 8 min each. The samples were then incubated with anti-mouse or anti-rabbit secondary antibodies, used at a dilution ratio of 1:1000, in a 37 °C incubator for 2 h. The samples were washed three times with warm PBS, for 8 min each. An anti-fluorescence quenching sealing agent (ProLong Gold Antifade Reagent, Cell Signaling Technology) was added to the samples, the pictures of which were taken using a confocal microscope.

CCK-8 test

CCK-8 is a highly sensitive kit that is widely used to detect cell proliferation and toxicity. The cells were seeded at a density of 1000 cells/well into 96-well plates. Culture plates were pre-cultured at 37 °C in a humidified incubator containing 5% CO_2, following which 10 mL of CCK-8 was added to each well, and the 96-well plates were placed in an incubator for 1–4 h. The readings were taken by measuring the absorbance at a wavelength of 450 nm.

Lactate dehydrogenase detection

Lactate dehydrogenase (LDH) is an enzyme present in cells. When cells are stimulated or damaged, LDH is released from inside the cell to the outside. Thus, LDH levels are usually measured to evaluate the degree of apoptosis or necrosis. The principle of this experiment involves the conversion of lactic acid into pyruvate upon catalysis by LDH, accompanied by the reduction of NAD+ to nicotinamide adenine diphosphate hydride (NADH), which then reacts with 2-p-iodophenyl-3-p-nitrophenyl-5-phenyltetrazolum chloride (INT) to produce trichromate methyl. This reaction leads to the generation of an absorption peak at a wavelength of 490 nm, which allows for the detection of LDH by means of colorimetry.

Cells in good condition were seeded into 96-well plates, at a density of 150 µL/well, and detected when the cell density reached 80%–85%. The old culture medium was then discarded, the cells rinsed with PBS, and a new culture medium added. After the pre-set time, the supernatant was aspirated and centrifuged for about 5 min at 300 g, following which the supernatant (120 µL) was added to the next culture plate and the readings were immediately determined.

ROS detection

ROS, including hydroxyl radicals, hydrogen peroxide, superoxide, and singlet oxygen, can damage nucleic acids and biofilms. Dichlorofluorescein diacetate (DCFH-DA) itself has no fluorescence, but can freely penetrate the cell membrane, to transform into DCFH inside the cells. ROS promotes the oxidation of DCFH to produce fluorescent substances. The levels of green fluorescence intensity were measured to estimate the level of intracellular ROS.

The cells were inoculated into 12-well plates with small slides, following which different drugs were added to the respective groups, and the cells were cultured for 72 h. When the cell density reached approximately 70%, DCFH-DA was directly added to the cells and they were incubated in the dark for 1 h, after reaching the initial concentration. The cells were then rinsed with PBS to remove residual DCFH-DA and reduce the background. The cells were observed and photographed under a fluorescence microscope and then collected and analyzed using flow cytometry.

Detection of apoptosis using flow cytometry

Annexin V, a phospholipid-binding protein, has high affinity for phosphatidylserine. It binds to the cell membranes of early apoptotic cells through the phosphatidylserine that is exposed outside these cells. Propidine iodide (PI) is a nucleic acid dye. However, in the middle and late stages of apoptosis and death, PI can penetrate the cell membrane and stain the nucleus red. Therefore, by matching the staining of annexin-V with PI, cells in the early and late stages of apoptosis can be detected.

The cells of each group were collected, re-suspended in the culture medium, and centrifuged at 4 °C for 5 min at 300 g, following which the supernatant was discarded. Pre-cooled PBS (1 mL) was then added to the cells, gently mixed, and then centrifuged at 400 g and 4 °C for 5 min. Post centrifugation, the supernatant was discarded, and the cells were re-suspended in 200 µL of PBS, to which 10 µL of fluorescein isothiocyanate (FITC)-annexin V and 10 µL of PI were added, gently mixed, and incubated at 4 °C in the dark for 30 min. PBS (300 µL) was then added to this system, followed by detection using flow cytometry. NovoExpress analysis software (Agilent) was used for the analysis.

Cell cycle detection using flow cytometry

The combination of PI and double-stranded DNA can produce fluorescence, the intensity of which is directly proportional to the double-stranded DNA content. After the DNA in the cell is stained with PI, the intracellular DNA content can be measured using flow cytometry, thereby helping in the analysis of the cell cycle.

We collected samples from each group. The collected cells (1×10^7) were re-suspended in 1 mL of medium and centrifuged at 400 g for 5 min, following which the supernatant was aspirated and discarded. The pellet was re-suspended in 300 µL of PBS, and 700 µL of anhydrous ethanol was added to it, following which this solution was placed in a refrigerator at -20 °C, to allow the cells to be fixed for more than 24 h. The fixed sample was then removed and centrifuged at 4 °C and 700 g for 5 min, following which the supernatant was aspirated and discarded. The cell pellet was washed twice with 1 mL of pre-cooled PBS, re-suspended in 0.5 mL of PI/RNase holding buffer, and incubated at room temperature for 15 min. The DNA content of the cells was measured using flow cytometry, to determine the proportion of cells in each cell cycle. The results were analyzed using NovoExpress software.

Histological analysis

Hematoxylin-eosin (HE) staining was used for the histological staining. Hematoxylin dye is alkaline, which mainly stains the chromatin in the nucleus and ribosome in the cytoplasm purple-blue. Eosin is an acidic dye that mainly stains components in the cytoplasm and extracellular matrix red. Masson's trichrome is one of the main methods used to stain fibers in tissues. It stains muscle fibers red and collagen fibers blue, and thus, helps distinguish collagen fibers from muscle fibers. Histologically, periodic acid–Schiff (PAS) staining is mainly used to detect glycogen or other polysaccharide substances; it stains glycogen and neutral mucilage material red and the nucleus blue.

Heart tissue was fixed with 10% formalin buffer, dehydrated with alcohol, and embedded in paraffin. We took 5 µm sections and stained them with HE, Masson's trichrome, and PAS. Photographs were taken using an optical microscope, while an Application Suite image system (Leica) was used to document the relevant parts of the sample.

Detection of myocardial injury markers

The main function of SOD is to catalyze the disproportionation of superoxide anion free radicals to hydrogen peroxide and oxygen. Superoxide anion free radicals are the normal metabolites in organisms. Creatine kinase (CK) is a dimer composed of two subunits, M and B. CK-MB in the myocardium accounts for approximately 10%–32%, so it is a marker of myocardial injury and has specificity. The apoptosis- or necrosis-mediated destruction of the cell membrane structure causes enzymes in the cytoplasm, such as LDH, to be released into the culture medium, with stable enzyme activity. Thus, we tested these three indicators using kits, according to the steps described in the manufacturer's instructions.

Echocardiographic detection

The mice were intraperitoneally injected with 3% sodium pentobarbital (40 mg/kg). After reaching a state of mild anesthesia, they were fixed on the animal fixation plate in the supine position. The mice were then touched with fingers, for apical pulsation. The hair in the heart region was removed and an appropriate amount of coupling agent was applied to the heart. The anterior zone was measured using an echocardiogram (Philips). A 2–4 MHz ultrasound probe was placed on the left side of the sternum, to show the short-axis section of the left ventricle.

Statistical analysis

All data were analyzed using Prism 6.0 (GraphPad). For the measurement data, the variance homogeneity test was carried out first, followed by the unpaired two-tailed t, t', or rank-sum test, as needed. Statistical significance was set at $P < 0.05$.

RESULTS

A flow chart of the animal and cell experiments is shown in Supplementary Figure 1.

Establishment of a mouse model of DCM

After STZ was injected into the mice of the experimental group, the blood glucose levels of the mice in each group were measured regularly (Table 1). The fasting blood glucose levels of mice in the control group were in the normal range, whereas after 8 wk of STZ injection, the fasting blood glucose levels of mice in the model group increased significantly compared to those before the injection ($P < 0.001$) and those in the control group ($P < 0.001$), which confirmed the successful establishment of the diabetes mouse model. Long-axis ultrasound imaging and cardiac function measurement of the left ventricle showed that compared to those in the control group, there was a significant decrease ($P < 0.05$) in the left ventricular end diastolic diameter, left ventricular ejection fraction, and left ventricular fraction shortening in the STZ group, while the left ventricular end systolic diameter increased significantly ($P < 0.05$), which suggested decreased cardiac function (Figure 1A and Table 2). Upon detection of myocardial injury markers, as compared to those in the control group, the levels of LDH and CK-MB increased significantly ($P < 0.0001$) in the STZ group, while SOD decreased significantly ($P < 0.0001$), accompanied by the generation of a large amount of ROS ($P < 0.0001$), indicating that there was serious oxidative stress injury in the myocardial tissue of mice in the STZ group (Figure 1B and Table 3). HE staining showed that compared to those in the control group, the cells in the STZ group were disordered and hypertrophic, with obviously broken and dissolved myocardial fibers. Masson's staining showed that cardiomyocytes in the STZ group were hypertrophic and necrotic, and obvious fibrous tissue hyperplasia appeared in the myocardial stroma. PAS staining showed that glycogen vacuoles, mucus, and myocardial interstitial inflammatory cell infiltration increased in the STZ group (Figure 1C). The above results indicated that compared to that in the normal control group, the myocardial tissue in the STZ group had obvious pathological damage, which further confirmed that the DCM model was established successfully.

Apoptosis of cardiomyocytes in DCM mice

Cardiomyocyte apoptosis plays an important role in DCM pathogenesis. To explore the apoptosis of cardiomyocytes in the HG environment, we performed the following experiments: (1) The myocardial tissue of the two groups was made into cell suspensions and flow cytometry was performed on them, which showed that there was a significant increase ($P < 0.0001$) in the apoptotic rate of cardiomyocytes in the DCM model group (Figure 2A); (2) Western blot was used to detect the expression of apoptosis-related proteins in the myocardium, which was compared to that in the control group, and it was found that there was no significant difference in the level of cardiomyocyte apoptosis-related protein Bcl-2 in the DCM model group ($P > 0.05$), while the expression of Bax and CC3 increased significantly, and there was obvious apoptosis ($P < 0.01$) (Figure 2B); and (3) Immunofluorescence showed that there was a significant enhancement ($P < 0.01$) in the fluorescence intensity of CC3 in the DCM model group (Figure 2C).

Proliferation of cardiomyocytes in DCM mice

After the onset of DCM, calcium overload in cardiomyocytes and excessive energy consumption by mitochondria might lead to a decrease in the number of cells. In order to explore the proliferation of cardiomyocytes in the HG environment, we carried out the following experiments: (1) The results of flow cytometry showed that the ratio of myocardial cells in the G1 phase in the DCM model group increased significantly ($P < 0.01$), indicating that the proliferation of many cells in the G1 phase was blocked (Figure 3A); (2) The cell cycle-related proteins in the two groups were detected using Western blot, which showed that compared to those in the control group, the expression levels of PCNA and CyclinD1 decreased significantly in the DCM model group ($P < 0.01$) (Figure 3B); and (3) Immunofluorescence also showed that there was a significant decrease ($P < 0.01$) in the expression of PCNA in the myocardial tissue of mice in the model group (Figure 3C). These results suggested that cardiomyocyte proliferation was significantly inhibited.

Expression levels of TRPC6 and P-CAMKII proteins in the myocardium of DCM mice

To clarify the role of TRPC6 in high glucose-induced cardiomyocyte injury, we detected the expression of TRPC6 and its related P-CaMKII signaling pathway in DCM mice. The myocardial tissues in the control and DCM model groups were analyzed using Western blot. Compared to those in the control group, the expression levels of calcium channel proteins, such as TRPC6 and P-CAMKII, increased significantly ($P < 0.01$) in the DCM model group (Figure 4A). The myocardial tissues of the two groups were analyzed using immunofluorescence, the results of which showed that there was a significant increase ($P < 0.001$) in the expression of TRPC6 in the myocardium of the model group (Figure 4B).

Table 1 Blood glucose levels in control and streptozotocin injection groups (mmo/L)

Group	n	0 wk	1 wk	4 wk	8 wk	12 wk
Control	10	6.3 ± 0.6	6.8 ± 0.6	6.7 ± 0.5	6.5 ± 0.3	6.4 ± 0.9
STZ	10	6.1 ± 0.5	16.1 ± 8.2	14.6 ± 3.8	19.2 ± 5.7[a,b]	23.4 ± 4.3[a,b]

[a]$P < 0.001$, compared with that before modeling.

[b]$P < 0.001$, compared with the control group.

STZ: Streptozotocin.

Table 2 Comparison of cardiac ultrasound results between control and streptozotocin injection groups in left ventricular end diastolic diameter, left ventricular end systolic diameter, left ventricular ejection fraction, and fraction shortening

Group	n	LVEDD (mm)	LVESD (mm)	LVEF (%)	LVFS (%)
Control	10	2.9 ± 0.4	0.95 ± 0.3	82 ± 2.1	67 ± 2.9
STZ	10	3.6 ± 0.3[a]	0.81 ± 0.5[a]	69 ± 3.2[b]	48 ± 1.8[c]

Compared with the control group:

[a]$P < 0.05$.

[b]$P < 0.01$.

[c]$P < 0.001$.

STZ: Streptozotocin; LVEDD: Left ventricular end diastolic diameter; LVESD: Left ventricular end systolic diameter; LVEF: Left ventricular ejection fraction; LVFS: Left ventricular fraction shortening.

Table 3 Detection of myocardial injury markers in control and streptozotocin injection groups

| Group	n	LDH (mU/mg)	CK-MB (U/g)	SOD (U/mg)
Control	10	424.7 ± 5.2	11.3 ± 0.5	67.5 ± 2.3
STZ	10	1027.6 ± 4.3[a]	48.2 ± 0.6[a]	19.8 ± 1.2[a]

Compared with the control group:

[a]$P < 0.0001$.

STZ: Streptozotocin; LDH: Lactate dehydrogenase; SOD: Superoxide dismutase.

Effects of SAR7334 and KN-93 on the pathological and biochemical changes of HG-induced H9C2 cardiomyocytes

To clarify the role and mechanism of TRPC6 and CaMKII in DCM-induced cardiomyocyte injury, H9C2 cardiomyocytes were treated with HG, to simulate DCM-induced cardiomyocyte injury *in vitro*. At the same time, the cells were pre-treated with SAR7334, a TRPC6 inhibitor, and KN-93, a CaMKII inhibitor, to evaluate their roles in HG-induced cardiomyocyte injury. Compared to the LG and control groups, the HG group displayed obvious cell necrosis and floating, with a significant decrease ($P < 0.05$) in the number of cells. In addition, compared to the HG group, there was alleviation of cell necrosis and a significant increase ($P < 0.05$) in the number of cells in the SAR7334 and KN-93 treatment groups, which suggested that the inhibition of TRPC6 and CaMKII might lessen HG-induced cardiomyocyte injury. The absorbance of each group at the wavelength of 450 nm was detected using the CCK-8 method, to evaluate the H9C2 cell proliferation in each group. The results showed that compared to the LG and control groups, there was a significant decrease ($P < 0.01$) in the viability of cells in the HG group (33 mmol/L), while the viabilities of cells in the HG + SAR and HG + KN-93 groups were significantly higher than those in the HG group ($P < 0.05$) (Figure 5A). LDH is widely distributed in the myocardium and brain, and participates in redox reactions in the cytoplasm. The amount of LDH released and mortality of cardiomyocytes are commonly used to evaluate the degree of cardiomyocyte injury. The OD value is an index that reflects LDH activity. Upon examination of LDH activity and cardiomyocyte mortality, compared to those in the control and LG groups, the OD value of cells increased significantly in the HG group, while the HG-induced LDH release was significantly inhibited in the HG + SAR and HG + KN-93 groups. Compared to those of the control and LG groups, the cell mortality of the HG group increased significantly, while compared to that of the HG group, the cell mortalities of the HG + SAR and HG + KN-93 groups decreased significantly (Figure 5B). Excessive ROS can cause serious
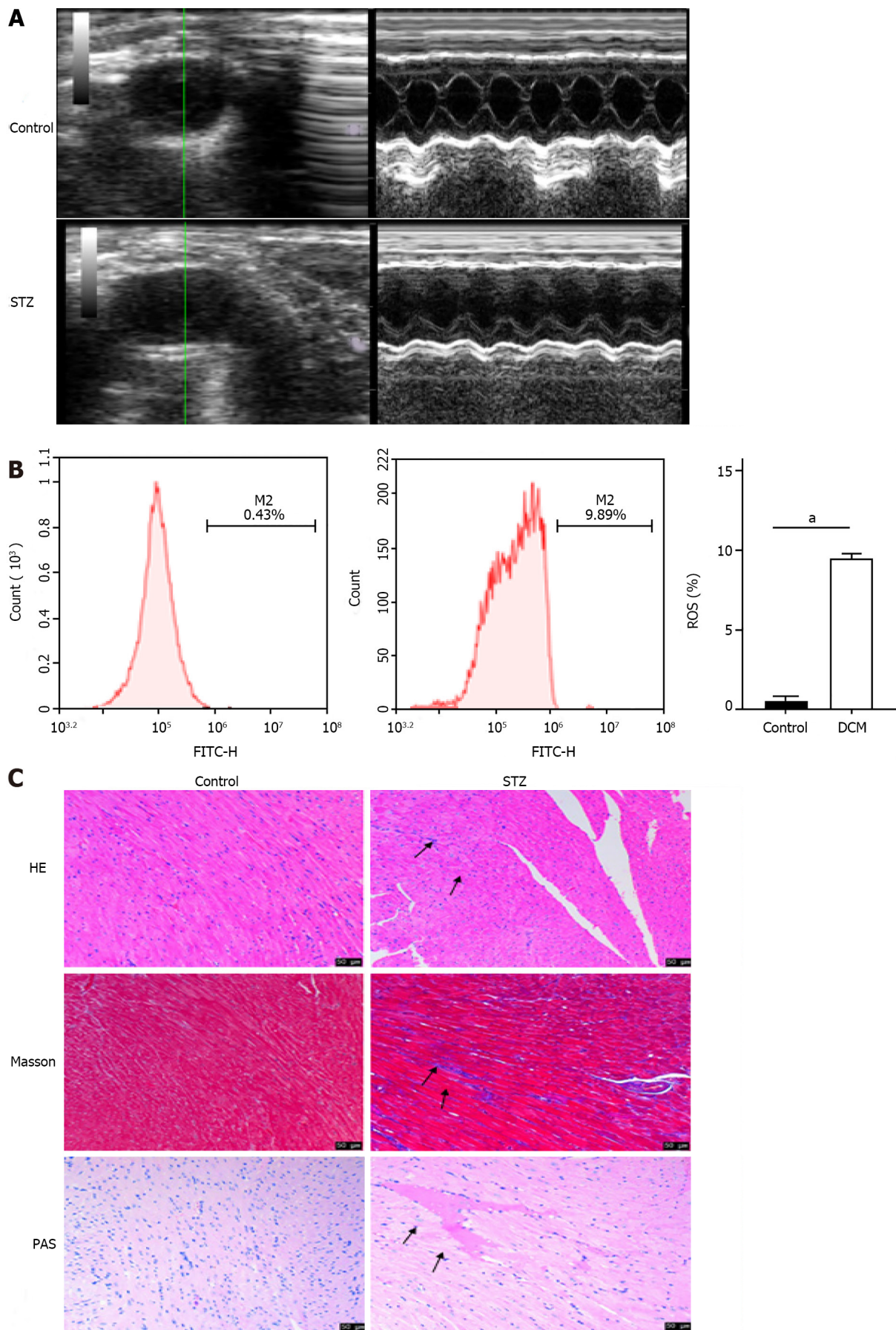
Figure 1 Long axis ultrasound imaging and cardiac function measurement of the left ventricle. A: Left ventricular short axis view and cardiac

function were measured in the control group and streptozotocin (STZ) injection group; B: Flow cytometry of reactive oxygen species in the control group and STZ injection group; C: HE, Masson, and periodic acid Schiff staining of diabetic cardiomyopathy and control mice. Scale bars = 50 μm. [a]$P < 0.0001$. STZ: Streptozotocin; ROS: Reactive oxygen species; PAS: Periodic acid Schiff.
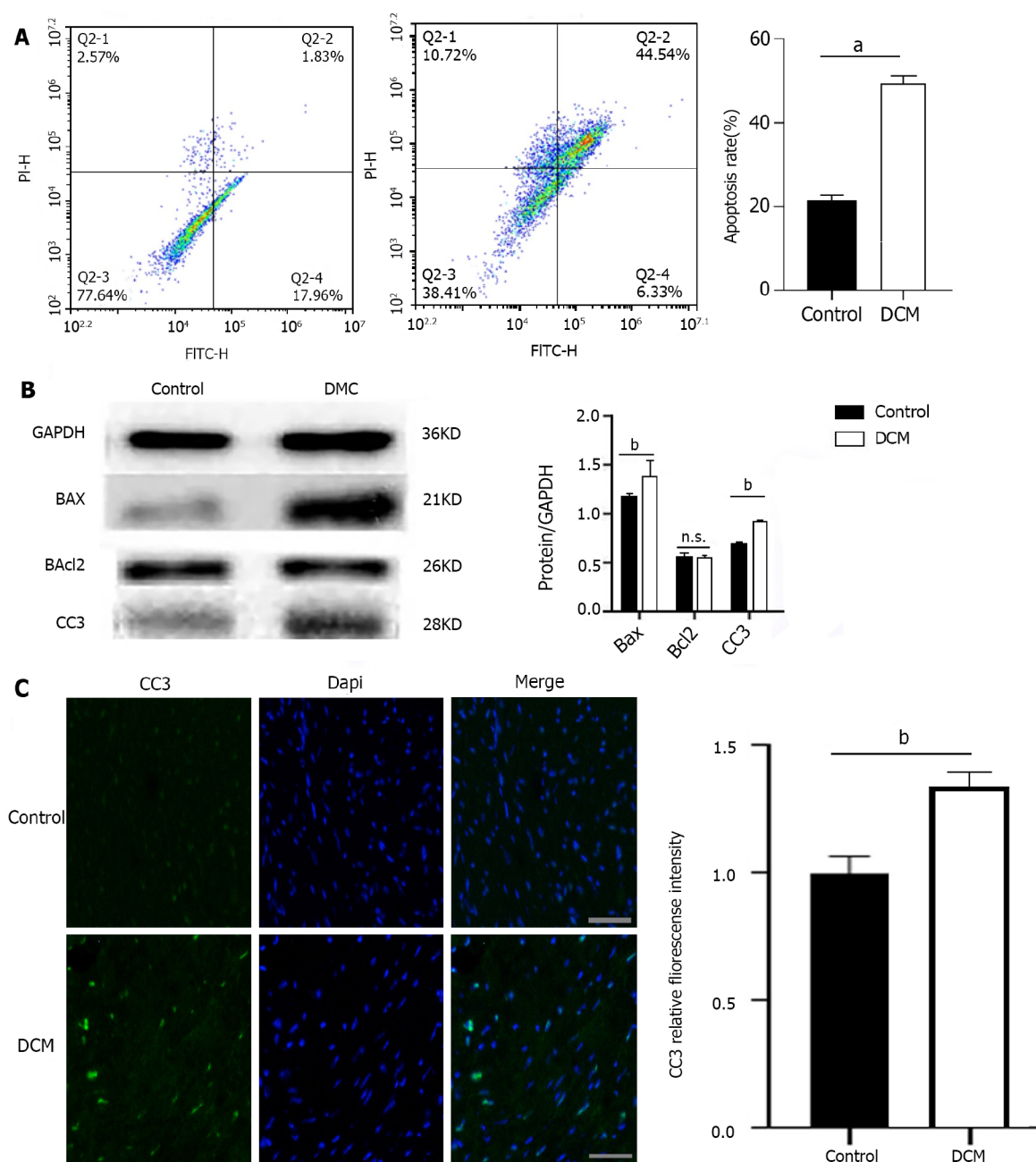
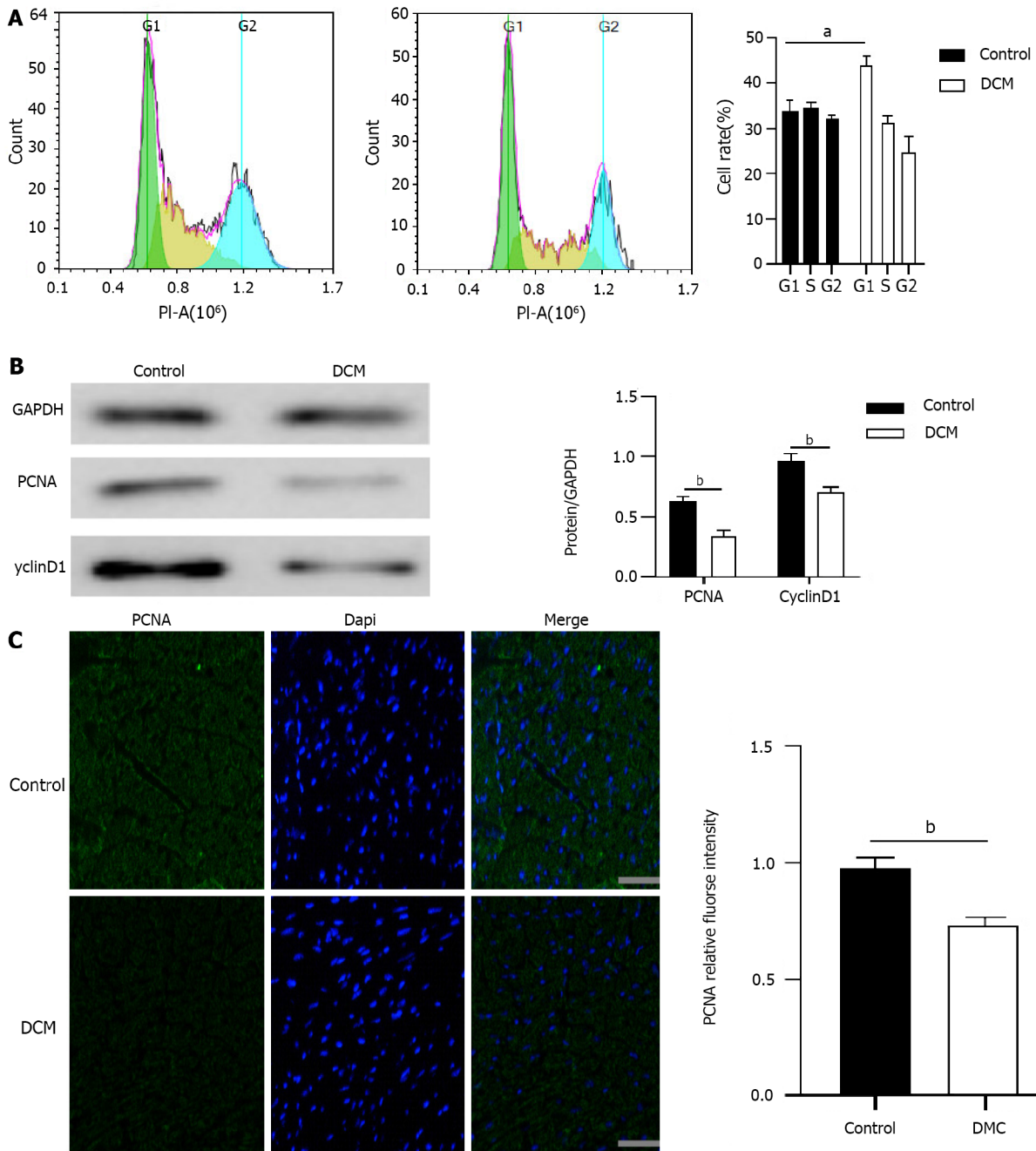DOI: 10.4239/wjd.v13.i4.338 **Copyright** ©The Author(s) 2022.

Figure 2 Apoptosis of cardiomyocytes in diabetic cardiomyopathy mice. A: Apoptosis of diabetic cardiomyopathy (DCM) and control mice was detected using double staining of FITC-Annexin V and propidine iodide and the representative images of flow cytometry are presented. [a]$P < 0.0001$; B: Expression levels of apoptosis related proteins BAX, cleaved Caspase 3 (CC3), and Bcl2 in DCM mice and control mice. $n = 5$, unpaired t-test, [b]$P < 0.01$. n.s.: No statistical difference; C: Fluorescence intensity of CC3 in cardiac myocytes of DCM and control mice. Scale bars = 20 μm, [b]$P < 0.01$. DCM: Diabetic cardiomyopathy.

damage to cytoplasmic proteins and nucleic acids, and is closely related to apoptosis. Upon detection of ROS fluorescence using DCFH-DA, the fluorescence intensity of the HG group was found to be significantly higher than those of the LG and control groups ($P < 0.0001$), while the levels of ROS in the cardiomyocytes of the HG + SAR and HG + KN-93 groups decreased significantly ($P < 0.0001$) (Figure 5C).

Effects of SAR7334 and KN-93 on HG-induced apoptosis of H9C2 cells
In order to further clarify whether the decline of cardiomyocyte viability induced by HG is related to

Figure 3 Proliferation of cardiomyocytes in diabetic cardiomyopathy mice. A: Cell cycle was detected by flow cytometry for the percentage of cells in each cell cycle of diabetic cardiomyopathy (DCM) and control mice. n = 5, unpaired t-test, [a]$P < 0.001$; B: The expression levels of cardiac cell cycle related proteins PCNA and CyclinD1 in DCM and control mice. n = 5, unpaired t-test, [b]$P < 0.01$; C: Fluorescence intensity of PCNA in cardiac myocytes of DCM and control mice. Scale bars = 20 μm, [b]$P < 0.01$. DCM: Diabetic cardiomyopathy.

mediation of apoptosis, we induced the cells using HG (33 mmoL/L) for 72 h and then detected the apoptosis of cells in each group using flow cytometry. Compared to those in the LG and control groups, the apoptosis rate was significantly higher ($P < 0.0001$) in the HG group; however, upon treatment with SAR (2 μmoL/L) and KN-93 (5 μmoL/L), as compared to that in the HG group, the apoptosis rates in the HG + SAR and HG + KN-93 groups decreased significantly ($P < 0.0001$) (Figure 6A). Moreover, when Western blot was used to detect the changes in the levels of apoptosis-related proteins including Bax, CC3, and Bcl-2 upon induction with HG, the expression levels of Bax and CC3 were found to be significantly up-regulated ($P < 0.001$), indicating that the H9C2 cells showed obvious apoptosis. However, compared to those in the HG group, the levels of Bax and CC3 proteins decreased significantly in the HG + SAR and HG + KN-93 groups ($P < 0.001$) (Figure 6B). Immunofluorescence results showed that the fluorescence intensity of CC3 increased significantly in the HG group ($P < 0.001$), while it decreased significantly ($P < 0.01$) in the HG + SAR and HG + KN-93 groups (Figure 6C and D). These results suggested that the effects of SAR7334 and KN-93 are similar, and that they both

DOI: 10.4239/wjd.v13.i4.338 **Copyright** ©The Author(s) 2022.
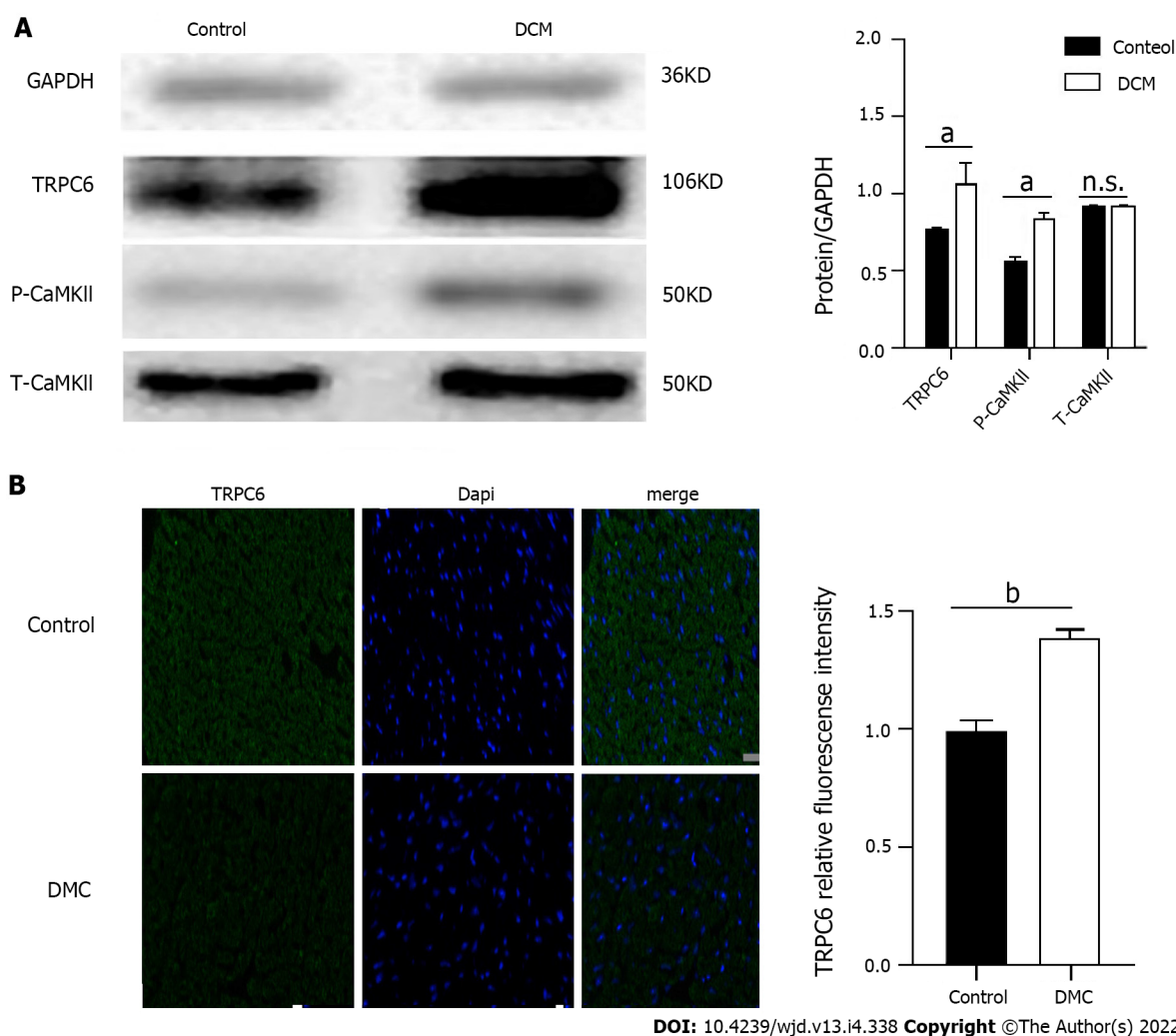
Figure 4 Expression of transient receptor potential channel 6 and P-CAMKII proteins in the myocardium of diabetic cardiomyopathy mice. A: Expression levels of calcium channel protein transient receptor potential channel 6 (TRPC6) and P-CAMKII in cardiac myocytes of diabetic cardiomyopathy (DCM) and control mice. n = 5, unpaired t-test, [a]P < 0.01. n.s.: No statistical difference; B: Fluorescence intensity of TRPC6 in cardiac myocytes of DCM and control mice. Scale bars = 20 μm, [b]P < 0.001. DCM: Diabetic cardiomyopathy; TRPC6: Transient receptor potential channel 6.

inhibit HG-induced apoptosis and protect cardiomyocytes.

Effects of SAR7334 and KN-93 on HG-induced inhibition of H9C2 cell proliferation

In order to further explore whether calcium overload can inhibit the proliferation of cardiomyocytes, we detected the cell cycle in different treatment groups using flow cytometry. Compared to those in the LG and control groups, the ratio of cells in G1 phase was significantly higher (P < 0.001) in the HG group, while as compared to that in the HG group, the ratio of cells in G1 phase was significantly lower (P < 0.01) in the HG + SAR7334 and HG + KN-93 groups (Figure 7A). In addition, when the expression levels of PCNA and CyclinD1 were detected using Western blot, as compared to those in the LG and control groups, the expression levels of PCNA and CyclinD1 were significantly down-regulated (P < 0.0001) in the HG group, while as compared to those in the HG group, the expression levels of PCNA and CyclinD1 were significantly up-regulated in the HG + SAR7334 and HG + KN-93 groups (P < 0.001) (Figure 7B). The results of immunofluorescence showed that as compared to those in the LG and control groups, there was a significant decrease (P < 0.0001) in the PCNA fluorescence intensity in the HG group, while as compared to that in the HG group, groups that were treated with SAR7334 and KN-93 displayed a significant increase (P < 0.01) in PCNA fluorescence intensity (Figure 7C and D). These results showed that calcium overload inhibited cell proliferation, but the cell proliferation improved upon addition of SAR7334 and KN-93.

Changes in TRPC6 and P-CAMKII expression upon intervention with SAR7334 and KN-93

In order to explore the specific mechanism of cardiomyocyte injury caused by HG, Western blot was used to detect the expression of TRPC6 and P-CAMKII in the different treatment groups. As compared to those in the LG and control groups, there was a significant increase (P < 0.001) in the expression
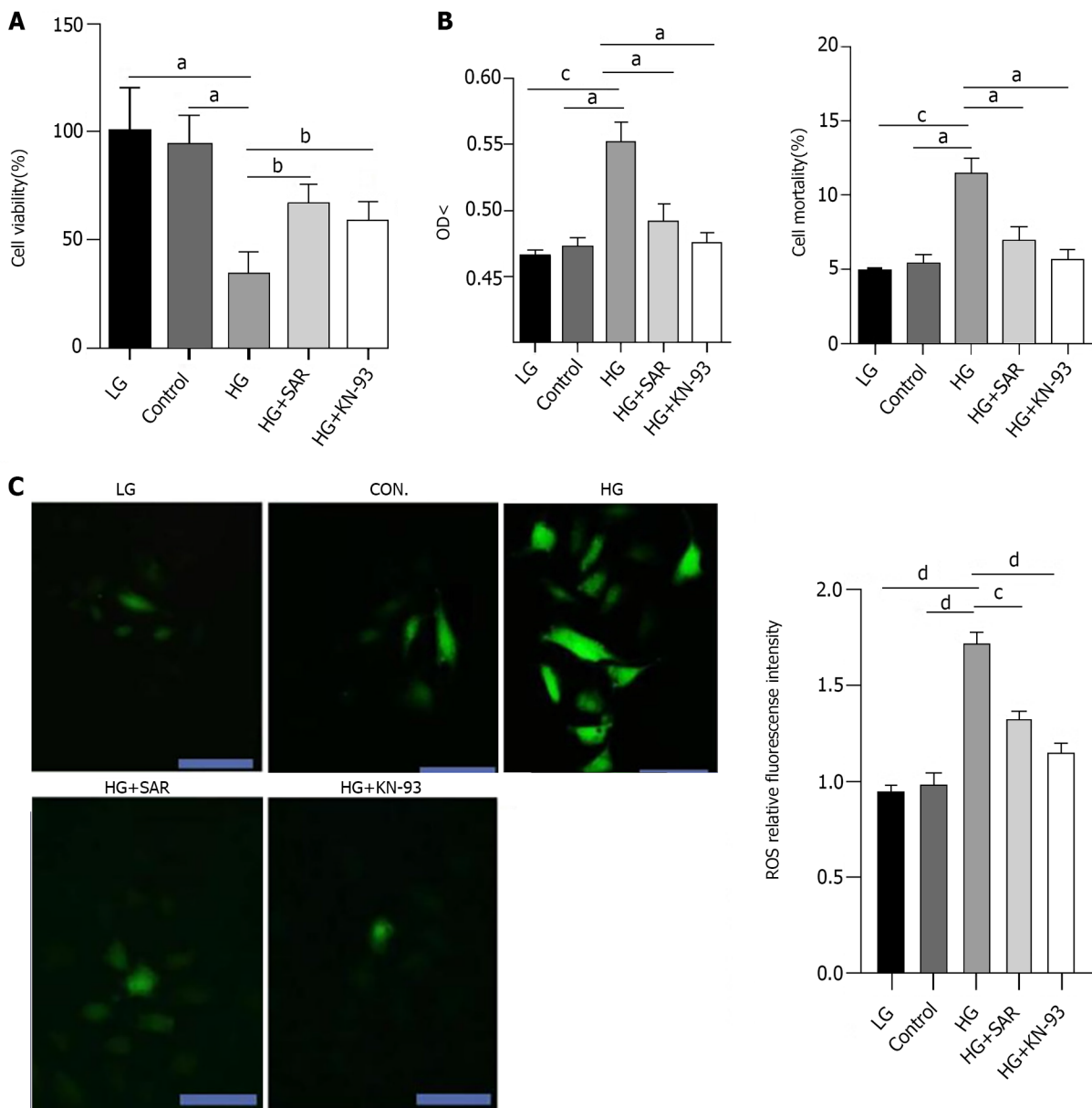
Figure 5 Pathological and biochemical changes of H9C2 cardiomyocytes in each group. A: After high glucose induced injury of H9C2 cells, the effects of SAR7334 and KN-93 on the proliferation of H9C2 cells were observed by Cell Counting Kit-8 method. [a]$P < 0.01$, [b]$P < 0.05$; B: After high glucose induced injury of H9C2 cells, lactate dehydrogenase method was used to detect the effects of SAR and KN-93 on the mortality of H9C2 cells. $n = 5$, unpaired t-test, [a]$P < 0.01$, [c]$P < 0.001$; C: Reactive oxygen species fluorescence intensity of each group after treatment with fluorescent probe DCFH-DA. $n = 5$, unpaired t-test, scale bars = 20 μm, [c]$P < 0.001$, [d]$P < 0.0001$. HG: High-glucose; LG: Low-glucose.

levels of TRPC6 and P-CAMKIl in the HG group, while compared to those in the HG group, there was a significant decrease ($P < 0.001$) in the expression levels of TRPC6 and P-CAMKIl in the HG + SAR and HG + KN-93 groups (Figure 8A). Immunofluorescence also showed that, as compared to those in the LG and control groups, there was a significant increase ($P < 0.0001$) in the fluorescence intensity of TRPC6 in the HG group, while the same decreased significantly ($P < 0.0001$) upon addition of SAR7334 and KN-93, suggesting that HG might activate the TRPC6/P-CAMKIl pathway, cause intracellular calcium overload, and finally result in cardiomyocyte injury (Figure 8B and C).

DISCUSSION

Normal metabolic function is important for maintaining homeostasis of the internal environment and normal functioning of various organs. Metabolic dysfunction can cause pathophysiological changes, from the level of the tissue cells to that of the whole body, through various mechanisms, such as imbalance of internal environment homeostasis, activation of inflammatory pathways, and activation of
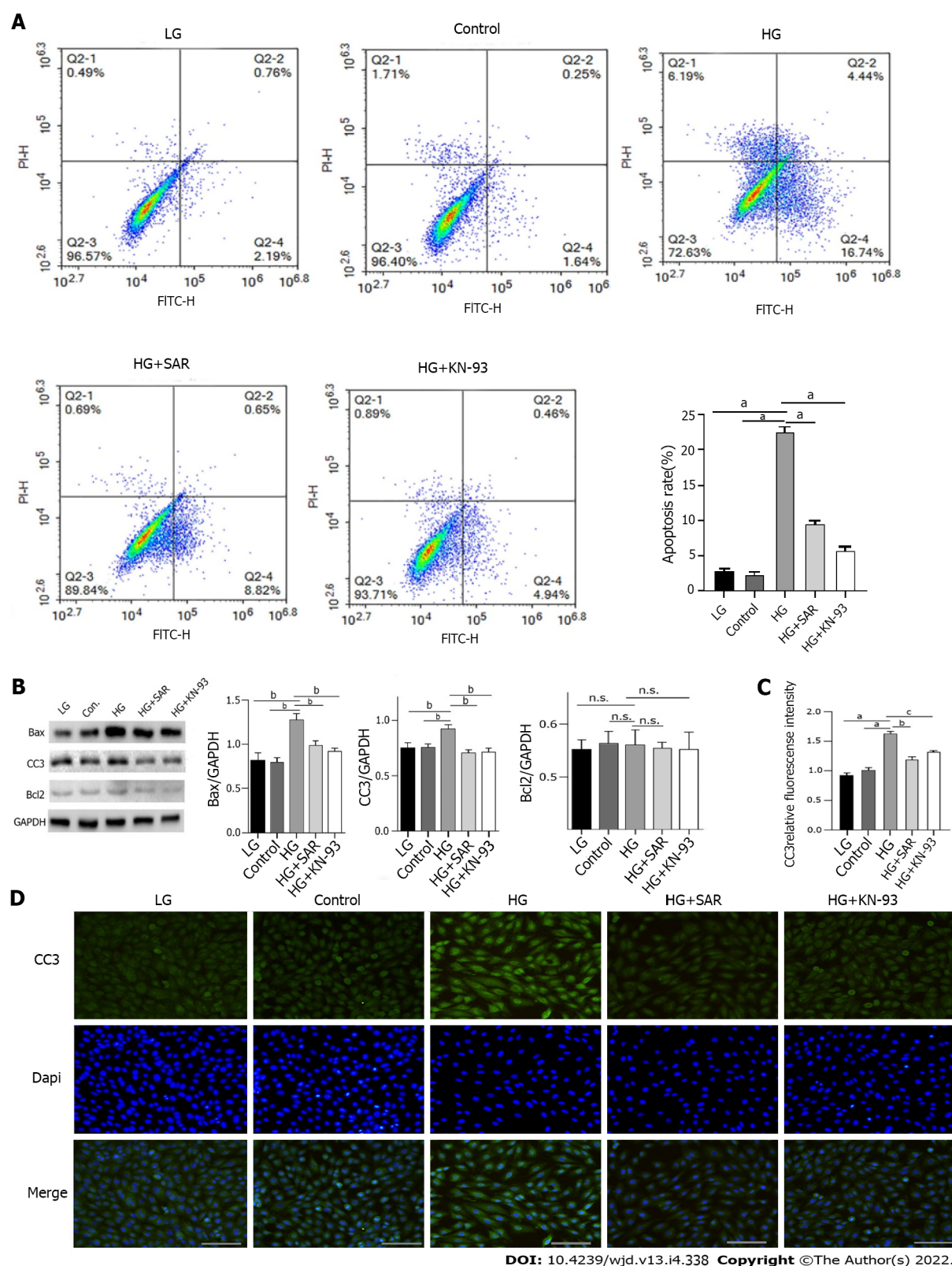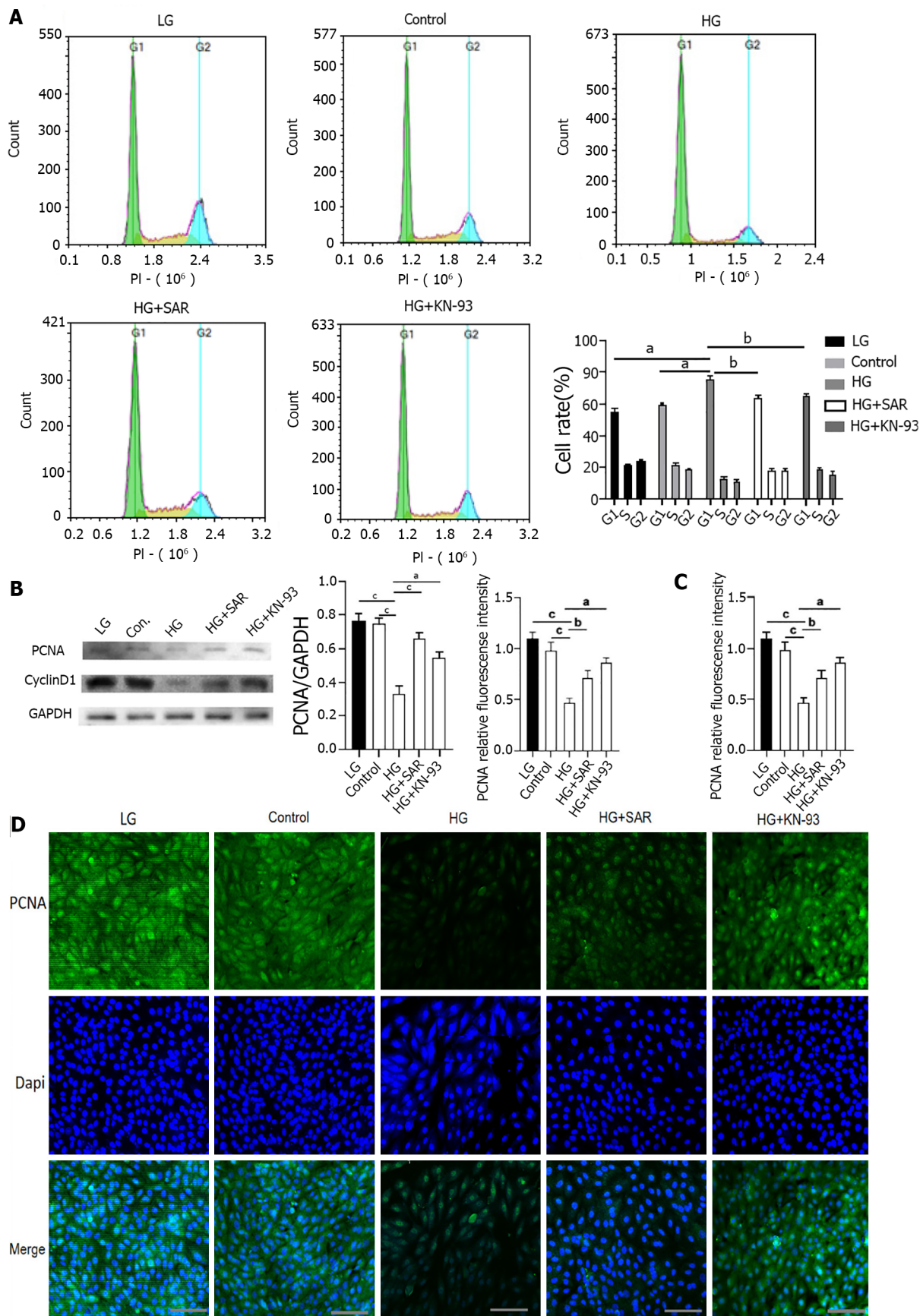
Figure 6 Effects of SAR7334 and KN-93 on high-glucose-induced apoptosis of H9C2 cells. A: Apoptosis rate of H9C2 cells in each group was detected by flow cytometry. $n = 5$, unpaired t-test, [a]$P < 0.0001$; B: Effects of SAR7334 and KN-93 on the expression of apoptosis related proteins Bax, cleaved Caspase 3 (CC3), and Bcl2 in H9C2 cells induced by high glucose. $n = 5$, unpaired t-test, [b]$P < 0.001$. n.s.: No statistical difference; C and D: Expression of apoptosis protein CC3 detected by immunofluorescence. $n = 5$, unpaired t-test, [a]$P < 0.0001$, [b]$P < 0.001$, [c]$P < 0.01$. Scale bars = 10 μm. HG: High-glucose; LG: Low-glucose.

apoptosis-related pathways[25-27]. Diabetes is caused by congenital genetic or acquired pathogenic factors. It manifests as a series of metabolic syndromes that are characterized by abnormal blood glucose elevation[28,29]. Diabetes usually leads to the activation of signaling pathways such as HIPPO/YAP [30], NF-κB/NLRP3[31], and Erk/Nrf2/HO-1[32], which leads to pathological changes in peripheral blood vessels, smooth muscles, and cardiomyocytes, manifested as diabetic foot, diabetic nephropathy,

DOI: 10.4239/wjd.v13.i4.338 **Copyright** ©The Author(s) 2022.

Figure 7 Effects of SAR7334 and KN-93 on high-glucose-induced inhibition of H9C2 cell proliferation. A: Percentage of cells in each group in each period was detected by flow cytometry. $n = 5$, unpaired t-test, [a]$P < 0.001$, [b]$P < 0.01$; B: Effects of SAR7334 and KN-93 on the expression levels of cycle related proteins PCNA and CyclinD1 in H9C2 cells induced by high glucose. $n = 5$, unpaired t-test, [a]$P < 0.001$, [b]$P < 0.01$, [c]$P < 0.0001$. n.s.: No statistical difference; C and D:

Expression of PCNA detected by immunofluorescence. n = 5, unpaired t-test, [a]P < 0.001, [b]P < 0.01, [c]P < 0.0001. Scale bars = 10 µm. HG: High-glucose; LG: Low-glucose.
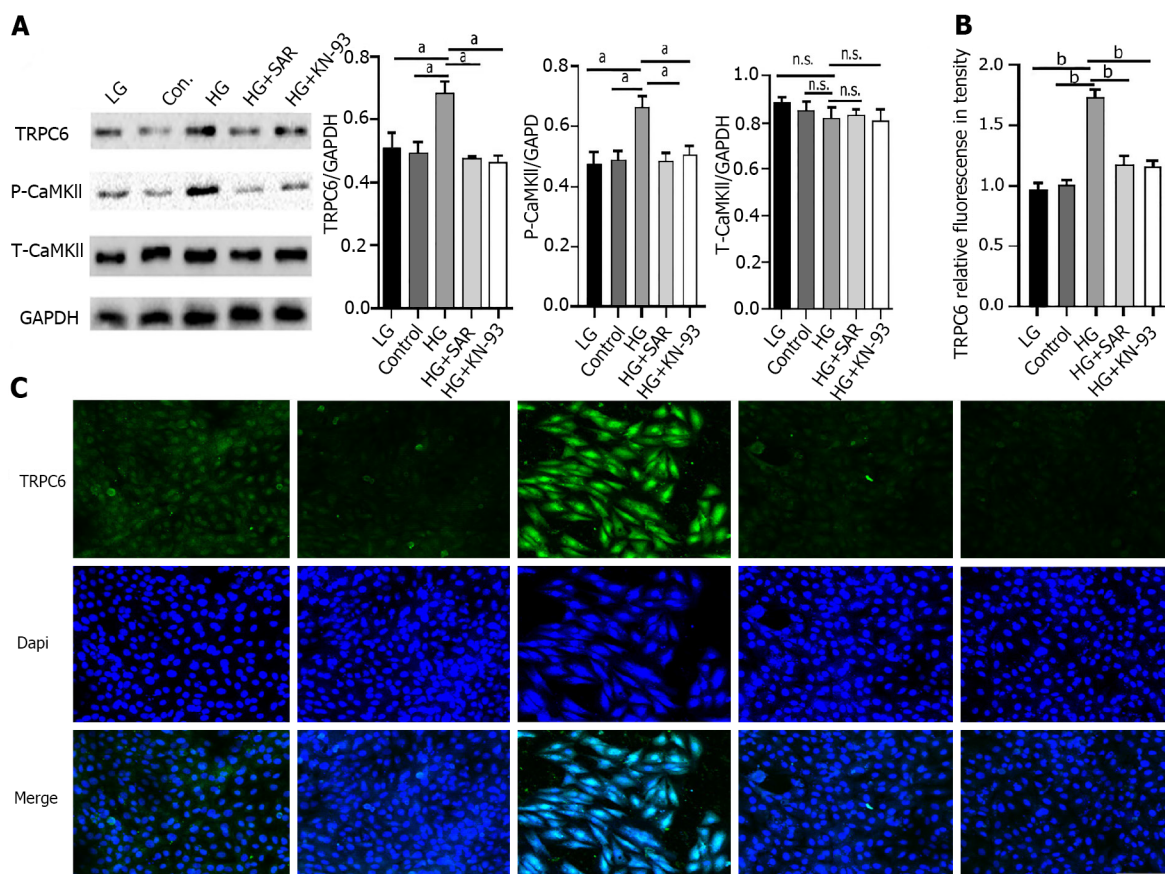
Figure 8 Changes of expression of transient receptor potential channel 6 (TRPC6) and P-CaMKII under the intervention of SAR7334 and KN-93. A: Effects of SAR7334 and KN-93 on the expression of transient receptor potential channel 6 (TRPC6) and P-CaMKII in high glucose induced H9C2 cells. n = 5, unpaired t-test, [a]P < 0.001. n.s.: No statistical difference; B and C: Expression of TRPC6 protein detected by immunofluorescence. n = 5, unpaired t-test, [b]P < 0.0001. Scale bars = 10 µm. HG: High-glucose; LG: Low-glucose; TRPC6: Transient receptor potential channel 6.

DCM, and other complications. Such complications cause an increase in the mortality rate of the patients [33-36]. DCM is a serious complication of diabetes[37] that is characterized by irreversible damage to myocardial structure and function in diabetic patients, due to hyperglycemia and metabolic disorders [38]. In terms of pathogenesis, studies have shown that DCM is an independent and specific myocardial injury, and the pathogenesis of DCM is different from that of hypertensive heart disease, coronary atherosclerotic heart disease, and other heart diseases[39,40]. Our present study suggests that HG levels might activate inflammatory pathways, to induce apoptosis and fibrous tissue proliferation in diabetic patients, thus playing an important role[41,42].

TRPC6 is a non-selective cation channel protein. It has been reported that TRPC6 can regulate Ca^{2+} influx under physiological conditions. *In vitro*, Sonneveld *et al*[43] found that the HG environment caused up-regulation of TRPC6 expression in an AngII expression-dependent manner[43]. Zhang *et al* [44] found that AngII could up-regulate the expression of TRPC6 in podocytes, increase Ca^{2+} influx, and promote podocyte apoptosis and autophagy[44]. Studies have shown that when the expression of TRPC6 increases, the intracellular Ca^{2+} concentration increases, resulting in the activation of calmodulin (CaM) and translocation of nuclear factor for activated T cells 2 (NFAT2) in the cytoplasm to the nucleus, which binds to the corresponding homeopathic elements in the target gene promoter, to trigger the expression of downstream molecules[45]. Elucidating the exact mechanism of TRPC6 in DCM pathogenesis has important theoretical and practical significance for the development of relevant therapeutic targets. This study aimed to explore the role of TRPC6 in the pathogenesis of DCM, using STZ to construct the DCM model and simulate the HG environment of cells *in vitro*.

In the present study, a DCM model was constructed by means of intraperitoneal injection of STZ. To clarify whether STZ can induce DCM effectively, we used HE, Masson's trichrome, and PAS pathological staining to detect changes in myocardial structure after modeling. Our results showed that

compared to the control group, there was an increase in cardiomyocyte hypertrophy/necrosis, collagen fiber proliferation, and glycogen vacuoles in the STZ group. This suggests that STZ could effectively induce DCM. To clarify the mechanism of STZ-induced DCM-related phenomena and to determine if it involved cardiomyocyte apoptosis, we performed flow cytometry, Western blot, and immunofluorescence, and found that in the STZ-injected group, there was a significant increase in the apoptosis rate, in addition to a significant increase in the expression of Bax and CC3 as well as fluorescence intensity of CC3, suggesting that the HG environment might aggravate the degree of cardiomyocyte apoptosis. The same experimental method was also used to detect the cell cycle, the results for which showed that in the model group, the ratio of cardiomyocytes in the G1 phase significantly increased, while the expression of PCNA and CyclinD1 as well as the PCNA fluorescence intensity of cardiomyocytes decreased obviously, which suggested that HG might inhibit the proliferation of cardiomyocytes. The expression levels of TRPC6 and P-CaMKII were also detected and found to be significantly higher in the model animals, as compared to those in the controls, suggesting that HG might promote cardiomyocyte apoptosis by activating the expression of TRPC6 and P-CaMKII.

Pathological oxidative stress and metabolic dysfunction can mediate cardiomyocyte injury through activation of the RAS and ROS systems[46]. Studies have shown that the activation of the ROS signaling pathway is an important mechanism of cell injury[46,47]. It has been reported that the production of intracellular ROS can directly damage the mitochondrial membrane and cause mutations in mitochondrial DNA, resulting in an imbalance between oxidative stress and Ca^{2+} regulation[47]. At the same time, ROS can also activate nuclear factor-kappaB (NF-κB) indirectly, such as by activating caspase-3 and its activator, thereby inducing the high expression of apoptosis-related genes[48]. As a non-selective calcium channel, TRPC6 can induce cell injury through calcium overload[49]. To further clarify the specific roles of TRPC6 in DCM, we examined the effect of TRPC6 on cardiomyocytes in the HG environment using *in vitro* cell culture experiments.

Under a light microscope, we found that there was severe apoptosis of H9C2 cells in a HG environment. SAR7334 and KN-93 are specific inhibitors of TRPC6 and CaMKII, respectively. Upon addition of SAR7334 and KN-93, there was alleviation of cell injury. The CCK-8 assay showed that SAR7334 and KN-93 had a protective effect on cardiomyocytes. LDH is widely distributed in the myocardium and brain, and participates in redox reactions in the cytoplasm. The amount of LDH released and mortality of cardiomyocytes are commonly used to evaluate the degree of cardiomyocyte injury. By detecting the LDH level in the supernatant of cultured cells, we confirmed that inhibition of CaM could alleviate the toxic effects of HG on cardiomyocytes. DCFH-DA was used to detect ROS. It was found that under HG stimulation, compared to that of the HG group, the content of ROS in cardiomyocytes of the HG + SAR and HG + KN-93 groups decreased significantly, indicating that the production of ROS is very important in the process of HG-induced apoptosis, which is regulated by the concentration of Ca^{2+}. The activation of TRPC6 induced by HG further caused intracellular calcium overload and increased the expression of CaM, which was the initiating factor leading to apoptosis; in addition, the ROS downstream further activated the apoptosis pathway.

To clarify whether HG can induce the apoptosis and proliferation inhibition of cardiomyocytes and elucidate the related pathways, we used flow cytometry, Western blot, and immunofluorescence to detect the rate of apoptosis, cell cycle, and expression of apoptosis-/cell cycle-related proteins. In the HG group, the apoptosis rate increased significantly, in addition to which, a greater number of cells were also blocked in the G1 phase. After application of SAR and KN-93, there was a decrease in the apoptosis rate, as well as the proportion of cells that were blocked in the G1 phase. The expression of apoptosis-related proteins, including Bax and CC3, increased significantly in the HG group, with the expression of TRPC6 and P-CaMKII showing the same trend. The expression of cell cycle-related proteins, including PCNA and cyclinD1, decreased significantly in the HG group, but improved upon addition of calcium channel inhibitors. These results suggested that the change in Ca^{2+} concentration might play an important role in this situation.

CONCLUSION

In conclusion, the results of the flow cytometry, immunofluorescence, and Western blot experiments suggested that the HG environment might lead to cardiomyocyte apoptosis and inhibition of cardiomyocyte proliferation, by inducing the TRPC6/P-CaMKII pathway. The *in vitro* experiments further validated that inhibition of TRPC6 and CaMKII might protect cells in the HG environment, improve cell activity, reduce cell mortality, and promote cell proliferation.

ARTICLE HIGHLIGHTS

Research background

Diabetic cardiomyopathy (DCM) is a serious complication of end-stage diabetes that presents symptoms

such as cardiac hypertrophy and heart failure. The transient receptor potential channel 6 (TRPC6) protein is a very important selective calcium channel that is closely related to the development of various cardiomyopathies.

Research motivation

In recent years, many studies have reported that calmodulin-dependent protein kinase II (CaMKII) plays an important role in various myocardial diseases, such as myocardial hypertrophy, myocardial infarction, and arrhythmia. However, there are few reports on the interaction between TRPC6 and CaMKII, which warrants further research.

Research objectives

The purpose of this study was to explore whether TRPC6 affects cardiomyocyte apoptosis and proliferation inhibition in DCM.

Research methods

We compared cardiac function and myocardial pathological changes in wild-type mice and mice injected with streptozotocin (STZ), in addition to comparing the expression of TRPC6 and P-calmodulin-dependent protein kinase II (P-CaMKII) in them. At the same time, we treated H9C2 cardiomyocytes with high glucose and then evaluated the effects of addition of SAR, a TRPC6 inhibitor, and KN-93, a CaMKII inhibitor, to such H9C2 cells in a high-glucose environment.

Research results

We found that STZ-treated mice had DCM, decreased cardiac function, necrotic cardiomyocytes, and limited proliferation. Western blot and immunofluorescence were used to detect the expression levels of various appropriate proteins in the myocardial tissue of mice and H9C2 cells. Compared to those in the control group, the expression levels of the apoptosis-related proteins cleaved caspase 3 and Bax were significantly higher in the experimental group, while the expression of the proliferation-related proteins proliferating cell nuclear antigen and CyclinD1 were significantly lower. *In vivo* and *in vitro*, the expression of TRPC6 and P-CaMKII increased in a high-glucose environment. However, addition of inhibitors to H9C2 cells in a high-glucose environment resulted in alleviation of both apoptosis and proliferation inhibition.

Research conclusions

The inhibition of apoptosis and proliferation of cardiomyocytes in a high-glucose environment may be closely related to activation of the TRPC6/P-CaMKII pathway.

Research perspectives

This study might provide a new insight for the treatment of DCM.

FOOTNOTES

Author contributions: Jiang SJ conceived and designed the study, collected, analyzed, and interpreted the data, wrote the manuscript, provided critical revisions that are important for the intellectual content, and approved the final version of the manuscript.

Institutional review board statement: This study was conducted with approval from the Ethics Committee of Hubei Provincial Center for Disease Control and Prevention (No. 202110009).

Institutional animal care and use committee statement: All animal experiments conformed to the internationally accepted principles for the care and use of laboratory animals.

Conflict-of-interest statement: There are no relevant financial or non-financial interests to disclose.

Data sharing statement: No additional data are available.

ARRIVE guidelines statement: The authors have read the ARRIVE guidelines, and the manuscript was prepared and revised according to the ARRIVE guidelines.

REFERENCES

1　**Wu X**, Huang L, Zhou X, Liu J. Curcumin protects cardiomyopathy damage through inhibiting the production of reactive oxygen species in type 2 diabetic mice. *Biochem Biophys Res Commun* 2020; **530**: 15-21 [PMID: 32828278 DOI: 10.1016/j.bbrc.2020.05.053]

2　**Ma C**, Luo H, Liu B, Li F, Tschöpe C, Fa X. Long noncoding RNAs: A new player in the prevention and treatment of diabetic cardiomyopathy? *Diabetes Metab Res Rev* 2018; **34**: e3056 [PMID: 30160026 DOI: 10.1002/dmrr.3056]

3　**Jammal Addin MB**, Young D, McCarrison S, Hunter L. Dilated cardiomyopathy in a national paediatric population. *Eur J Pediatr* 2019; **178**: 1229-1235 [PMID: 31187263 DOI: 10.1007/s00431-019-03404-w]

4　**Barison A**, Grigoratos C, Todiere G, Aquaro GD. Myocardial interstitial remodelling in non-ischaemic dilated cardiomyopathy: insights from cardiovascular magnetic resonance. *Heart Fail Rev* 2015; **20**: 731-749 [PMID: 26423909 DOI: 10.1007/s10741-015-9509-4]

5　**Gasparini S**, Fonfara S, Kitz S, Hetzel U, Kipar A. Canine Dilated Cardiomyopathy: Diffuse Remodeling, Focal Lesions, and the Involvement of Macrophages and New Vessel Formation. *Vet Pathol* 2020; **57**: 397-408 [PMID: 32125251 DOI: 10.1177/0300985820906895]

6　**Griffin TP**, Wall D, Browne GA, Dennedy MC, O'Shea PM. Associations between glycaemic control and activation of the renin-angiotensin-aldosterone system in participants with type 2 diabetes mellitus and hypertension. *Ann Clin Biochem* 2018; **55**: 373-384 [PMID: 28814103 DOI: 10.1177/0004563217728964]

7　**Climent M**, Viggiani G, Chen YW, Coulis G, Castaldi A. MicroRNA and ROS Crosstalk in Cardiac and Pulmonary Diseases. *Int J Mol Sci* 2020; **21** [PMID: 32575472 DOI: 10.3390/ijms21124370]

8　**Xu J**, Ismat FA, Wang T, Lu MM, Antonucci N, Epstein JA. Cardiomyocyte-specific loss of neurofibromin promotes cardiac hypertrophy and dysfunction. *Circ Res* 2009; **105**: 304-311 [PMID: 19574548 DOI: 10.1161/CIRCRESAHA.109.201509]

9　**Dendorfer A**, Dominiak P, Schunkert H. ACE inhibitors and angiotensin II receptor antagonists. *Handb Exp Pharmacol* 2005; 407-442 [PMID: 16596809 DOI: 10.1007/3-540-27661-0_15]

10　**Li T**, Li D, Xu H, Zhang H, Tang D, Cao H. Wen-Xin Decoction ameliorates vascular endothelium dysfunction *via* the PI3K/AKT/eNOS pathway in experimental atherosclerosis in rats. *BMC Complement Altern Med* 2016; **16**: 27 [PMID: 26803585 DOI: 10.1186/s12906-016-1002-7]

11　**Phosri S**, Arieyawong A, Bunrukchai K, Parichatikanond W, Nishimura A, Nishida M, Mangmool S. Stimulation of Adenosine A_{2B} Receptor Inhibits Endothelin-1-Induced Cardiac Fibroblast Proliferation and α-Smooth Muscle Actin Synthesis Through the cAMP/Epac/PI3K/Akt-Signaling Pathway. *Front Pharmacol* 2017; **8**: 428 [PMID: 28713274 DOI: 10.3389/fphar.2017.00428]

12　**Zhao J**, Posa DK, Kumar V, Hoetker D, Kumar A, Ganesan S, Riggs DW, Bhatnagar A, Wempe MF, Baba SP. Carnosine protects cardiac myocytes against lipid peroxidation products. *Amino Acids* 2019; **51**: 123-138 [PMID: 30449006 DOI: 10.1007/s00726-018-2676-6]

13　**An D**, Rodrigues B. Role of changes in cardiac metabolism in development of diabetic cardiomyopathy. *Am J Physiol Heart Circ Physiol* 2006; **291**: H1489-H1506 [PMID: 16751293 DOI: 10.1152/ajpheart.00278.2006]

14　**Boyer JK**, Thanigaraj S, Schechtman KB, Pérez JE. Prevalence of ventricular diastolic dysfunction in asymptomatic, normotensive patients with diabetes mellitus. *Am J Cardiol* 2004; **93**: 870-875 [PMID: 15050491 DOI: 10.1016/j.amjcard.2003.12.026]

15　**Santoni G**, Morelli MB, Marinelli O, Nabissi M, Santoni M, Amantini C. Calcium Signaling and the Regulation of Chemosensitivity in Cancer Cells: Role of the Transient Receptor Potential Channels. *Adv Exp Med Biol* 2020; **1131**: 505-517 [PMID: 31646523 DOI: 10.1007/978-3-030-12457-1_20]

16　**Dietrich A**, Chubanov V, Gudermann T. Renal TRPathies. *J Am Soc Nephrol* 2010; **21**: 736-744 [PMID: 20395377 DOI: 10.1681/ASN.2009090948]

17　**Yue D**, Wang Y, Xiao JY, Wang P, Ren CS. Expression of TRPC6 in benign and malignant human prostate tissues. *Asian J Androl* 2009; **11**: 541-547 [PMID: 19701218 DOI: 10.1038/aja.2009.53]

18　**Müller M**, Essin K, Hill K, Beschmann H, Rubant S, Schempp CM, Gollasch M, Boehncke WH, Harteneck C, Müller WE, Leuner K. Specific TRPC6 channel activation, a novel approach to stimulate keratinocyte differentiation. *J Biol Chem* 2008; **283**: 33942-33954 [PMID: 18818211 DOI: 10.1074/jbc.M801844200]

19　**Ilatovskaya DV**, Palygin O, Chubinskiy-Nadezhdin V, Negulyaev YA, Ma R, Birnbaumer L, Staruschenko A. Angiotensin II has acute effects on TRPC6 channels in podocytes of freshly isolated glomeruli. *Kidney Int* 2014; **86**: 506-514 [PMID: 24646854 DOI: 10.1038/ki.2014.71]

20　**Zhang Y**, Zhang K, Ma L, Gu H, Li J, Lei S. Fluoride induced endoplasmic reticulum stress and calcium overload in ameloblasts. *Arch Oral Biol* 2016; **69**: 95-101 [PMID: 27280945 DOI: 10.1016/j.archoralbio.2016.05.015]

21　**Sun YH**, Li YQ, Feng SL, Li BX, Pan ZW, Xu CQ, Li TT, Yang BF. Calcium-sensing receptor activation contributed to apoptosis stimulates TRPC6 channel in rat neonatal ventricular myocytes. *Biochem Biophys Res Commun* 2010; **394**: 955-961 [PMID: 20307499 DOI: 10.1016/j.bbrc.2010.03.096]

22   **Pasch E**, Muenz TS, Rössler W. CaMKII is differentially localized in synaptic regions of Kenyon cells within the mushroom bodies of the honeybee brain. *J Comp Neurol* 2011; **519**: 3700-3712 [PMID: 21674485 DOI: 10.1002/cne.22683]

23   **Zhao L**, Cheng G, Jin R, Afzal MR, Samanta A, Xuan YT, Girgis M, Elias HK, Zhu Y, Davani A, Yang Y, Chen X, Ye S, Wang OL, Chen L, Hauptman J, Vincent RJ, Dawn B. Deletion of Interleukin-6 Attenuates Pressure Overload-Induced Left Ventricular Hypertrophy and Dysfunction. *Circ Res* 2016; **118**: 1918-1929 [PMID: 27126808 DOI: 10.1161/CIRCRESAHA.116.308688]

24   **Kraft L**, Erdenesukh T, Sauter M, Tschöpe C, Klingel K. Blocking the IL-1β signalling pathway prevents chronic viral myocarditis and cardiac remodeling. *Basic Res Cardiol* 2019; **114**: 11 [PMID: 30673858 DOI: 10.1007/s00395-019-0719-0]

25   **Hu H**, Tian M, Ding C, Yu S. The C/EBP Homologous Protein (CHOP) Transcription Factor Functions in Endoplasmic Reticulum Stress-Induced Apoptosis and Microbial Infection. *Front Immunol* 2018; **9**: 3083 [PMID: 30662442 DOI: 10.3389/fimmu.2018.03083]

26   **Wehrwein EA**, Orer HS, Barman SM. Overview of the Anatomy, Physiology, and Pharmacology of the Autonomic Nervous System. *Compr Physiol* 2016; **6**: 1239-1278 [PMID: 27347892 DOI: 10.1002/cphy.c150037]

27   **Slominski AT**, Zmijewski MA, Semak I, Kim TK, Janjetovic Z, Slominski RM, Zmijewski JW. Melatonin, mitochondria, and the skin. *Cell Mol Life Sci* 2017; **74**: 3913-3925 [PMID: 28803347 DOI: 10.1007/s00018-017-2617-7]

28   **Muscogiuri G**, Barrea L, Annunziata G, Di Somma C, Laudisio D, Colao A, Savastano S. Obesity and sleep disturbance: the chicken or the egg? *Crit Rev Food Sci Nutr* 2019; **59**: 2158-2165 [PMID: 30335476 DOI: 10.1080/10408398.2018.1506979]

29   **Bianchetti DGAM**, Amelio GS, Lava SAG, Bianchetti MG, Simonetti GD, Agostoni C, Fossali EF, Milani GP. D-lactic acidosis in humans: systematic literature review. *Pediatr Nephrol* 2018; **33**: 673-681 [PMID: 29218437 DOI: 10.1007/s00467-017-3844-8]

30   **Kalscheuer H**, Serfling G, Schmid S, Lehnert H. [Diabetic emergencies : Hypoglycemia, ketoacidotic and hyperglycemic hyperosmolar nonketotic coma]. *Internist (Berl)* 2017; **58**: 1020-1028 [PMID: 28849301 DOI: 10.1007/s00108-017-0317-x]

31   **Shu Z**, Gao Y, Zhang G, Zhou Y, Cao J, Wan D, Zhu X, Xiong W. A functional interaction between Hippo-YAP signalling and SREBPs mediates hepatic steatosis in diabetic mice. *J Cell Mol Med* 2019; **23**: 3616-3628 [PMID: 30821074 DOI: 10.1111/jcmm.14262]

32   **An Y**, Zhang H, Wang C, Jiao F, Xu H, Wang X, Luan W, Ma F, Ni L, Tang X, Liu M, Guo W, Yu L. Activation of ROS/MAPKs/NF-κB/NLRP3 and inhibition of efferocytosis in osteoclast-mediated diabetic osteoporosis. *FASEB J* 2019; **33**: 12515-12527 [PMID: 31461386 DOI: 10.1096/fj.201802805RR]

33   **Shopit A**, Niu M, Wang H, Tang Z, Li X, Tesfaldet T, Ai J, Ahmad N, Al-Azab M. Protection of diabetes-induced kidney injury by phosphocreatine *via* the regulation of ERK/Nrf2/HO-1 signaling pathway. *Life Sci* 2020; **242**: 117248 [PMID: 31899224 DOI: 10.1016/j.lfs.2019.117248]

34   **Koller A**, Szenasi A, Dornyei G, Kovacs N, Lelbach A, Kovacs I. Coronary Microvascular and Cardiac Dysfunction Due to Homocysteine Pathometabolism; A Complex Therapeutic Design. *Curr Pharm Des* 2018; **24**: 2911-2920 [PMID: 29938610 DOI: 10.2174/1381612824666180625125450]

35   **Tabas I**, Bornfeldt KE. Macrophage Phenotype and Function in Different Stages of Atherosclerosis. *Circ Res* 2016; **118**: 653-667 [PMID: 26892964 DOI: 10.1161/CIRCRESAHA.115.306256]

36   **Bandyk DF**. The diabetic foot: Pathophysiology, evaluation, and treatment. *Semin Vasc Surg* 2018; **31**: 43-48 [PMID: 30876640 DOI: 10.1053/j.semvascsurg.2019.02.001]

37   **Borghetti G**, von Lewinski D, Eaton DM, Sourij H, Houser SR, Wallner M. Diabetic Cardiomyopathy: Current and Future Therapies. Beyond Glycemic Control. *Front Physiol* 2018; **9**: 1514 [PMID: 30425649 DOI: 10.3389/fphys.2018.01514]

38   **Zhao L**, Dong M, Xu C, Zheng H, Wei T, Liu K, Yan Z, Gao H. Identification of Energy Metabolism Changes in Diabetic Cardiomyopathy Rats Using a Metabonomic Approach. *Cell Physiol Biochem* 2018; **48**: 934-946 [PMID: 30036879 DOI: 10.1159/000491960]

39   **Hu X**, Bai T, Xu Z, Liu Q, Zheng Y, Cai L. Pathophysiological Fundamentals of Diabetic Cardiomyopathy. *Compr Physiol* 2017; **7**: 693-711 [PMID: 28333387 DOI: 10.1002/cphy.c160021]

40   **Rao K R**, Reddy S, Kashyap JR, Ramalingam V, Dash D, Kadiyala V, Kumar S, Reddy H, Kaur J, Kumar A, Kaur N, Gupta A. Association of culprit lesion plaque characteristics with flow restoration post-fibrinolysis in ST-segment elevation myocardial infarction: an intravascular ultrasound-virtual histology study. *Egypt Heart J* 2020; **72**: 86 [PMID: 33296051 DOI: 10.1186/s43044-020-00121-w]

41   **Fogarassy G**, Vathy-Fogarassy Á, Kenessey I, Kásler M, Forster T. Risk prediction model for long-term heart failure incidence after epirubicin chemotherapy for breast cancer - A real-world data-based, nationwide classification analysis. *Int J Cardiol* 2019; **285**: 47-52 [PMID: 30905520 DOI: 10.1016/j.ijcard.2019.03.013]

42   **Wei H**, Bu R, Yang Q, Jia J, Li T, Wang Q, Chen Y. Exendin-4 Protects against Hyperglycemia-Induced Cardiomyocyte Pyroptosis *via* the AMPK-TXNIP Pathway. *J Diabetes Res* 2019; **2019**: 8905917 [PMID: 31886288 DOI: 10.1155/2019/8905917]

43   **Sonneveld R**, van der Vlag J, Baltissen MP, Verkaart SA, Wetzels JF, Berden JH, Hoenderop JG, Nijenhuis T. Glucose specifically regulates TRPC6 expression in the podocyte in an AngII-dependent manner. *Am J Pathol* 2014; **184**: 1715-1726 [PMID: 24731445 DOI: 10.1016/j.ajpath.2014.02.008]

44   **Zhang H**, Ding J, Fan Q, Liu S. TRPC6 up-regulation in Ang II-induced podocyte apoptosis might result from ERK activation and NF-kappaB translocation. *Exp Biol Med (Maywood)* 2009; **234**: 1029-1036 [PMID: 19546355 DOI: 10.3181/0901-RM-11]

45   **Yao XM**, Liu YJ, Wang YM, Wang H, Zhu BB, Liang YP, Yao WG, Yu H, Wang NS, Zhang XM, Peng W. Astragaloside IV prevents high glucose-induced podocyte apoptosis *via* downregulation of TRPC6. *Mol Med Rep* 2016; **13**: 5149-5156 [PMID: 27109610 DOI: 10.3892/mmr.2016.5167]

46   **Sun X**, Chen RC, Yang ZH, Sun GB, Wang M, Ma XJ, Yang LJ, Sun XB. Taxifolin prevents diabetic cardiomyopathy *in*

vivo and *in vitro* by inhibition of oxidative stress and cell apoptosis. *Food Chem Toxicol* 2014; **63**: 221-232 [PMID: 24269735 DOI: 10.1016/j.fct.2013.11.013]

47   **Wang Y**, Sun H, Zhang J, Xia Z, Chen W. Streptozotocin-induced diabetic cardiomyopathy in rats: ameliorative effect of PIPERINE *via* Bcl2, Bax/Bcl2, and caspase-3 pathways. *Biosci Biotechnol Biochem* 2020; **84**: 2533-2544 [PMID: 32892714 DOI: 10.1080/09168451.2020.1815170]

48   **Wang X**, Li S, Liu L, Jian Z, Cui T, Yang Y, Guo S, Yi X, Wang G, Li C, Gao T, Li K. Role of the aryl hydrocarbon receptor signaling pathway in promoting mitochondrial biogenesis against oxidative damage in human melanocytes. *J Dermatol Sci* 2019; **96**: 33-41 [PMID: 31543430 DOI: 10.1016/j.jdermsci.2019.09.001]

49   **Yokosawa T**, Yamada M, Noguchi T, Suzuki S, Hirata Y, Matsuzawa A. Pro-caspase-3 protects cells from polymyxin B-induced cytotoxicity by preventing ROS accumulation. *J Antibiot (Tokyo)* 2019; **72**: 848-852 [PMID: 31371783 DOI: 10.1038/s41429-019-0216-6]